# Chapter 8
# Observer-based calibration of a power-law model for head loss in pipelines

Lizeth Torres[1] and Cristina Verde[1]

**Abstract** This chapter presents a real-time approach based on a nonlinear state observer for estimating both the coefficient and the exponent of a power-law model for head loss in a pipeline. Such a power law is nothing but a generalization of conventional models such as the Darcy-Weisbach and the Hazen-William formulas. The interest in estimating the parameters of the power law is twofold: to avoid handling values of physical parameters that may be uncertain, such as relative roughness, and to have an appropriate model for computational pipeline monitoring applications, such as leak detection and localization. The real-time estimation is performed by a state observer from the following available information of the pipeline: a flow rate and two pressure head recordings. To demonstrate how the proposed approach works, the state observer was implemented in MATLAB and experimental data from a lab pipeline was used to feed it. In addition, numerical simulations of a leak location algorithm are presented to show how a well-calibrated head loss model is highly necessary for leak diagnosis.

## 8.1 Introduction

The proper management of pipelines and fluid distribution networks requires some tasks that should be preferably executed in real time, for example, the detection and identification of faults or the pressure control for minimizing fluid losses (Verde and Torres, 2017; Puig et al., 2017). Usually these tasks are performed by algorithms based on mathematical models that are formulated from physical principles. In addition, although these algorithms have been shown to work very well in practice, they have an intrinsic problem: they must be frequently updated because their governing equations are functions of physical parameters that evolve over time in a slow or drastic way according to the operational and environmental conditions. In particular, in pipelines that have been in service for a considerable time, there are two physical parameters that notably change: the roughness and the internal diameter. Both in fact can be related to a normalized parameter: the relative roughness.

Relative roughness varies because of the natural deterioration processes that affect the internal wall of the pipelines such as corrosion, erosion, tuberculation or the deposit of materials. Such a variation directly modifies the dissipation of energy between the wall and the fluid.

[1]Instituto de Ingeniería UNAM, Ciudad Universitaria, Coyoacán, 04510, Mexico, e-mail: ftorreso@iingen.unam.mx and verde@unam.mx

The total energy dissipation in a pipeline is the sum of two hydraulic losses: the quasi-steady and the unsteady losses (Adamkowski and Lewandowski, 2006). Several authors have tried to model the unsteady loss, which is present in fast transients, by proposing in parallel, models that match experimental data and methods to calibrate them. These models and the associated calibration methods, however, are not discussed here since the unsteady loss is out of the scope of this chapter. The reader may consult the reviews provided in Bergant et al. (2001) and Savic et al. (2009) to know more about the state-of-the-art research on this topic.

The quasi-steady loss, which is known as head loss or pressure drop, can be divided into two main classes: major losses, associated with energy loss caused by viscous friction in the pipeline wall, and minor losses, associated with bends, fittings and valves. The head loss can be then expressed as follows (White, 1999):

$$\Delta H(Q) = \Delta H_f(Q) + \sum_{i=1}^{N} \Delta H_m(Q), \tag{8.1}$$

where $Q$ is the flow rate in the pipeline, $\Delta H_f(Q)$ denotes the major losses and $\sum_{i=1}^{N} \Delta H_m(Q)$ represents the sum of the minor losses.

The conventional equations used to calculate the major losses are the Darcy-Weisbach (DW) equation together with more empirical formulas such as the Hazen-Williams (HW) and the Manning equations, which are power laws (Moore, 1959). The DW equation, however, is more accepted with respect to the empirical formulas because it is dimensionally homogeneous and applicable to water as well as to other fluids (Liou, 1998). The DW equation is expressed as follows:

$$\Delta H_f(Q) = f(Q)\frac{L}{\phi}\frac{Q^2}{2gA_r^2}, \tag{8.2}$$

where $f(Q)$ is the dimensionless friction factor, $L$ is the length of the pipeline, $\phi$ is the pipeline diameter, $A_r$ is the cross-sectional area and $g$ is the gravitational acceleration. Minor losses represent additional energy dissipation provoked by pipeline devices that act against the fluid and reduce its energy, velocity, or momentum.

The major and minor losses can also be simultaneously calculated with the DW equation, but the real length $L$ involved in the DW equation must be replaced by a equivalent length that depends on the flow rate and characteristics of the pipeline accessories (Chapter 2, Larock et al. (1999)).

As it can be seen, the DW equation is a function of the flow rate and other physical parameters such as the friction factor, which is also a function of the flow rate (through the Reynolds number) and additional parameters, such as the relative roughness and the kinematic viscosity. For laminar flow, the friction factor can be calculated by using the Hagen-Poiseuille law, which is very simple (Hitzer, 2001). Nevertheless, in real operating conditions, pipelines work in the turbulent flow, and the friction computation becomes more complicated. In such a case, the consensual way to calculate the friction factor is by using the Colebrook-White (CW) equation, which is an implicit formula for which many explicit approximations have been proposed (Brkić, 2011). A mutual problem of using the CW equation or its approximations, however, is that they require the current value of the relative roughness along the pipeline. The relative roughness can be measured in real time by using a profilometer (as seen in Farshad et al. (2001); Sletfjerding and Gudmundsson (2003)), but it is necessary to wait for the complete scan of

the pipeline's internal wall. This test can be quite lengthy if the pipe is long or difficult to access, which leads to considering better alternatives for avoiding the use of the actual value of the relative roughness.

An alternative is the calibration of a model for the head loss[1]. To perform this alternative, it is necessary to provide a calibration method (a parameter estimation method) and a model of the head loss (e.g., the DW equation or the HW formula) with parameters to be experimentally estimated.

The calibration problem remains an open problem. Currently, many researchers dedicate much effort in proposing more efficient and easy-to-tune methods to convince practitioners to use them. Recently in Kumar et al. (2010), the authors presented an approach to estimate the roughness coefficients of the pipelines of a network, which is based on a k-means clustering algorithm and on the theory of graphs. In the same year, the Battle of the Water Calibration Networks (BWCN) was conducted by 14 teams from academia, water utilities, and private consultants. The BWCN results were given at the 12th Annual Conference on Water Distribution Systems Analysis and presented in Ostfeld et al. (2011). More recently, in Gao (2017) a method based on weighted least squares (WLS) was presented to compute the Hazen-Williams C factors of pipelines. In Díaz et al. (2017), the authors proposed a method based on a multi-period state estimation and mathematical programming decomposition techniques. Additionally, they presented an analysis of the observability of the roughness from available measurements.

In this spirit, this contribution proposes a real-time approach based on a state observer for calibrating the coefficient and the exponent of a power law that models the head loss only as a function of the flow rate and not as a function of the relative roughness and other uncertain parameters. The proposed approach only requires a flow rate and pressure measurements. Therefore, this method can be used in trunk pipelines instrumented with pressure and flow rate sensors placed at locations such as pump stations, where these sensors are usually installed.

The benefits of proposing a power law to approximate the total head loss together with a method for calibrating it in real time are the following: (a) to have a head loss model that expresses a general representation of conventional formulas used to compute the head loss such as the HW, the Manning or the Valiantzas equations (Chapter 2, Larock et al. (1999), Chapter 2, Chaudhry (1979)); (b) to avoid using a complicated formula such as the CW equation, which is implicit because it requires iterative methods to be solved; (c) to have a valid model for a given operation region instead of formulas for describing the complete turbulent regimen; (d) to have an identifiable model, i.e., a model with a structure involving easily estimated parameters by means of real-time algorithms; (e) to have a differentiable function.

An essential requirement in applying our approach is that the flow in the pipeline must be excited to ensure the identifiability of the parameters. This means that the flow in the pipeline must be perturbed during a short period while the parameters are estimated. Therefore, in order to satisfy the excitation condition, a steady-oscillatory flow in the pipeline is induced by injecting a sinusoidal signal into the frequency drive of the supply pump. Many of the off-line methods for detecting leaks and identifying parameters proposed by the hydraulic community, which have been verified in a laboratory, are based on the induction of steady-oscillatory flow in a pipeline by the sinusoidal maneuver of a valve (Xu and Karney, 2017).

To estimate the parameters of power laws in the context addressed here, some approaches have been proposed: for instance, those presented in Datta and Sridharan (1994) and Reddy et al. (1996), which use least squares and information (pressure and flow rate) recorded during a prescribed period. Moreover,

[1] The parameter estimation process in a model is called the calibration process in hydraulics.

the reader can find in Savic et al. (2009) a masterful review of proposed methods to calibrate pipelines and networks. The authors of this review categorize the methods as steady-state and transient and discuss the advantages and drawbacks of each one.

The novelty of this contribution is an experimental validation and the improvement of the approach presented in Torres and Verde (2018), which in turn was inspired by early results from Rojas et al. (2018), where the real-time estimation of the coefficients of both a quadratic and a cubic equation that approximate the head loss in a pipeline is proposed.

## 8.2 Physical system and modeling

This section describes the characteristics of the pipelines for which the proposed method can be used. This section also presents the extended model (an auxiliary model) used for the design of the state observer that performs the parameter estimation. Such an auxiliary system is deduced from a mathematical model commonly used in hydraulic problems: the rigid water column (RWC) model (Cabrera et al., 1995; Nault and Karney, 2016), which in turn is deduced from physical principles.

### *8.2.1 Physical system*

The approach presented in this chapter works for pipelines that satisfy the following: unidirectional flow and constant cross-sectional area. Furthermore, such pipelines must be instrumented such that pressure head measurements at the ends of the pipeline are available, as well as a flow rate recording at any point of the pipeline.

### *8.2.2 Rigid water column model*

In this chapter, the model considered for representing the head loss in a pipeline is the power law $\Delta H = \Omega Q^{\gamma}$, where $\Omega$ and $\gamma \leq 2$ are parameters related to the friction losses and fluid properties.

Since the goal of this chapter is to propose a real-time method for experimentally estimating $\Omega$ and $\gamma$ by using a state observer, a dynamical model involving these parameters is needed. This model is the so-called RWC model, which describes the flow in one dimension by ignoring the compressibility of the fluid and the elasticity of the conduit such that the entire column of fluid is assumed to move as a rigid body. The RWC model can be used to describe short pipelines or small sections of long-distance pipelines. For describing the overall behavior of the flow in pressurized long-distance pipelines, the fluid should be considered as compressible or slightly compressible. By assuming slight compressibility, the model must be modified to consider the unsteady friction, which involves the pressure wave propagation velocity and pressure changes along the spatial domain. This is out of the scope of this chapter.

The RWC model for a pipeline without extractions is expressed by the following equation (Islam and Chaudhry, 1998; Nault and Karney, 2016):

$$\dot{Q} = \beta \Delta H - \alpha Q^{\gamma+1}, \tag{8.3}$$
$$y_m = Q,$$

where $y_m$ is the measured flow rate, $\beta$ and $\alpha$ are parameters with appropriate units of measure.

If $\dot{Q} = 0$, Eq. (8.3) becomes an expression for the head loss

$$\Delta H = \frac{\alpha}{\beta} Q^{\gamma+1}, \tag{8.4}$$

which, by defining $\Omega = \alpha/\beta$, becomes

$$\Delta H = \Omega Q^{\gamma+1}, \tag{8.5}$$

which is nothing but the head loss model to be updated experimentally in real-time. Therefore, to obtain an estimation of $\Omega$, $\alpha$ and $\beta$ must first be estimated.

Once $\Omega$ and $\gamma$ are estimated, these can be associated with the physical characteristics of both the pipeline and fluid by means of conventional formulas for head loss, e.g., the Darcy-Weisbach equation, the Hazen-Willian equation or the Gauckler–Manning–Strickler formula. If the Darcy-Weisbach is used for a pipeline with length $L$, then $\gamma = 1$ and $\Omega = f(Q)L/2g\phi A_r^2$.

## 8.3 Real-time calibration approach

In order to estimate $\alpha$, $\beta$ and $\gamma$ by using a state observer, these parameters can be considered as state variables and they are added to the state vector of the RWC model given by (8.3). The above results in an extended model that combines the equations governing the evolution of the original state and the equations describing the evolution of the parameters.

### *8.3.1 Extended model*

The extended model is obtained by defining the following states: $x_1 = -\ln(Q)$, $x_2 = \beta$, $x_3 = \alpha Q^{\gamma}$ and $x_4 = \gamma$. In addition, these states form the state vector $x = [x_1\ x_2\ x_3\ x_4]^T$. The resulting extended model reads as follows:

$$\dot{x} = \begin{pmatrix} 0 & -u_1 & 1 & 0 \\ 0 & 0 & 0 & 0 \\ 0 & 0 & 0 & 0 \\ 0 & 0 & 0 & 0 \end{pmatrix} x + \begin{pmatrix} 0 \\ 0 \\ x_3 x_4 u_2 \\ 0 \end{pmatrix},$$
$$y = \begin{pmatrix} 1\,0\,0\,0 \end{pmatrix} x, \tag{8.6}$$

where $u_1 = \Delta H/Q$ and $u_2 = \dot{Q}/Q$ are assumed to be the inputs that form the input vector $u = [u_1\ u_2]$ and the output variable is $x_1$.

**Remark 1**: The system given by Eq. (8.6) has the following general structure:

$$\begin{aligned} \dot{x} &= A(u)x + B(u,x), \\ y &= Cx, \end{aligned} \tag{8.7}$$

where $A(u) \in \mathbb{R}^{n\times n}$ depends only on inputs and $B(u,x) \in \mathbb{R}^{n\times 1}$ is a nonlinear vector with a triangular structure (Besançon, 2007).

Therefore, one proposes in the following paragraphs a state observer for a system with the structure given by Eq. (8.7).

### *8.3.2 State observer*

For the state estimation of extended dynamical systems with the form given by Eq. (8.7), it was proven in Torres et al. (2012) that with a specific excitation and under the usual technical (Lipschitz) assumption for a high-gain design, one can obtain an asymptotic estimation of the extended state with the following *high-gain* observer:

$$\begin{aligned} \dot{\hat{x}} &= A(u)\hat{x} + B(u,\hat{x}) + SC^T(y-\hat{y}), \\ \hat{y} &= C\hat{x}, \end{aligned} \tag{8.8}$$

where $\hat{x}$ is the estimated extended state vector, $u$ is the input vector, $y$ is the measured output, and $S$ is the solution of the Lyapunov equation

$$\dot{S} = \lambda S + [A(u) + dB_\lambda(u,\hat{x})]S + S[A(u) + dB_\lambda(u,\hat{x})]^T - SC^TCS, \tag{8.9}$$

where $\lambda$ is a parameter for adjusting the convergence rate and $dB_\lambda(u,\hat{x}) = \partial B(u,\hat{x})/\partial\hat{x}$ is the Jacobian of $B(u,\hat{x})$. Particularly, for system (8.6), the Jacobian reads as follows:

$$dB_\lambda(u,\hat{x}) = \frac{\partial B(u,\hat{x})}{\partial x} = \begin{pmatrix} 0\,0 & 0 & 0 \\ 0\,0 & 0 & 0 \\ 0\,0 & u_2\hat{x}_4 & u_2\hat{x}_3 \\ 0\,0 & 0 & 0 \end{pmatrix}. \tag{8.10}$$

**Remark 2**: Notice that $\hat{\alpha}$ can be obtained as $\alpha = \hat{x}_3/(-\exp(\hat{x}_1))^{\hat{x}_4}$.

**Remark 3**: Since the estimations of $\hat{\alpha}$, $\hat{\beta}$ and $\hat{\gamma}$ from the state observer are quantities that evolve over time and may contain both noise and unmodeled effects, the mean of these estimations must then be calculated once these estimations reach steady state in order to have a unique value: $\bar{\alpha}$, $\bar{\beta}$ and $\bar{\gamma}$. The variation of the estimates from the mean values can be calculated as follows: $e_\alpha = \bar{\alpha} - \hat{\alpha}$, $e_\beta = \bar{\beta} - \hat{\beta}$ and $e_\gamma = \bar{\gamma} - \hat{\gamma}$ to analyze the unmodeled effects.

A condition for the convergence of the estimation is that inputs $u_1$ and $u_2$ must be persistently exciting: they need to satisfy a persistent or excitation condition, which is complicated to fulfill in advance. Therefore, inputs are usually designed heuristically and checked afterwards. Recently, some optimization-based methods for characterizing the persistent inputs for a particular class of systems have been proposed; see Scola et al. (2018) for instance. These methods, however, need to be extended to other classes of nonlinear systems.

### 8.3.3 Persistent condition: Steady-oscillatory flow

In this contribution, to obtain inputs that satisfy the persistent condition, the procedure detailed in Besançon (2016) was used, which states that a persistent input may be chosen on the basis of the output derivatives' mapping. Therefore, the mapping for system (8.6) was calculated, which reads as follows:

$$\Phi(x(t),u(t),y(t)) = \begin{pmatrix} y(t) \\ \dot{y}(t) \\ \ddot{y}(t) \\ y^{(3)}(t) \end{pmatrix} = \begin{pmatrix} x_1 \\ -x_2u_1 + x_3 \\ -x_2\dot{u}_1 + x_3x_4u_2 \\ -x_2\ddot{u}_1 + x_3x_4^2u_2^2 + x_3x_4\dot{u}_2 \end{pmatrix}. \tag{8.11}$$

The mapping (8.11) becomes injective as soon as $u_1$, $u_2$ and their derivatives are nonzero. Therefore, for any input with period $T$, the excitation condition is validated in a time window given by the period $T$. Sinus-like pressure heads and flow rate are natural candidates for satisfying such an injectivity. Moreover, many of the off-line methods for detecting leaks and identifying parameters proposed by the hydraulic community, which have been verified in a laboratory, are based on the induction of steady-oscillatory flow in a pipeline by the sinusoidal maneuver of a valve (Xu and Karney, 2017).

### 8.3.4 Derivative of the flow rate measurement

For implementing the state observer (8.8), the derivative of the flow rate $Q$ measurement is required. To obtain such a derivative, the following two steps are proposed, taking into account both the periodic nature of the signal and the knowledge of its fundamental frequency.

1. Estimate on-line the Fourier coefficients that approximate the signal. This task can be achieved by using the following proposed observer, which is based on an auxiliary system.
   The first state of the auxiliary system (used for the observer design) is the integral of $Q$ expressed as the finite version of the Fourier series:

$$\nu_1(t) = \int_0^t \left[ \frac{a_0}{2} + \sum_{i=1}^{N} \left( a_i \cos(i\omega\tau) + b_i \sin(i\omega\tau) \right) \right] d\tau, \tag{8.12}$$

   where $N$ denotes the total number of the frequency components taken into account to approximate the signal $Q$.
   By defining the Fourier coefficients $a_0$, $a_i$ and $b_i$ as the rest of the states, the auxiliary system is defined as follows:

$$\dot{\nu} = \underbrace{\begin{pmatrix} 0\ 1 & \cos(\omega t) & \sin(\omega t) & \ldots & \cos(N\omega t) & \sin(N\omega t) \\ 0\ 0 & -\omega\sin(\omega t) & \omega\cos(\omega t) & \ldots & -N\omega\sin(N\omega t) & N\omega\cos(N\omega t) \\ \vdots & & & & & \vdots \\ 0\ 0 & -\omega^N\sin(\omega t) & \omega^N\cos(\omega t) & \ldots & -N^N\omega^N\sin(N\omega t) & N^N\omega^N\cos(N\omega t) \end{pmatrix}}_{A_\omega} \nu, \quad (8.13)$$

$$y_\omega = C_\omega \nu,$$

where the state vector $\nu \in \mathrm{R}^M$ and the output vector $C_\omega \in \mathrm{R}^M$ are, respectively, defined as

$$\nu = \left[\int_0^t Q \ \ a_0 \ \ a_1 \ \ b_1 \ \ \ldots \ \ a_N \ \ b_N\right]^T,$$

$$C_\omega = [1 \ \ 0 \ \ \ldots \ \ 0].$$

Furthermore, $M = 2N+2$ is the total number of states.

The states of system (8.13), i.e., the Fourier coefficients, can then be estimated by using the following state observer:

$$\dot{\hat{\nu}} = A_\omega \hat{\nu} + K_\omega e_\omega, \quad (8.14)$$

$$\hat{y}_\omega = C_\omega \hat{\nu}, \quad (8.15)$$

where $e_\omega = \int_0^t Q - \hat{y}_\omega$, $K_\omega = S_\omega C_\omega^T$ and $S_\omega$ is calculated with the Lyapunov equation

$$\dot{S}_\omega = \mu S_\omega + A_\omega S_\omega + S_\omega A_\omega^T - S_\omega (C_\omega^T C_\omega) S_\omega, \quad (8.16)$$

where $\mu$ is the parameter for manipulating the convergence rate.

Observer (8.14) was tuned: $\mu = 1$, $S_\omega(0) = I$, where $I$ is the identity matrix, the state initial conditions were chosen to be 0 and $N = 3$. This latter parameter was chosen in this way to consider only the more meaningful frequency components: the fundamental frequency and two harmonics.

2. Construct the derivative of $Q$ by using the estimated Fourier coefficients as follows:

$$\hat{\dot{Q}} = \sum_{i=1}^{N} \left(-\hat{a}_i i\omega \sin(i\omega t) + \hat{b}_i i\omega \cos(i\omega t)\right), \quad (8.17)$$

where $N = 3$.

Thus, by using the two estimators (8.8) and (8.14), the implementation to obtain the parameters of the power law is summarized in the scheme given in Fig. 8.1.

## 8.4 Experiments

The results described below were obtained during experimental tests developed in a pipeline located at II-UNAM. A layout of the pipeline and its physical parameters are presented in Fig. 8.2 and Table 8.1, respectively. The installation consists of a storage tank of 10 [$m^3$] and a spiral loop on the vertical plane that returns the water to the tank. In addition, a servo valve is connected at the end of the line to

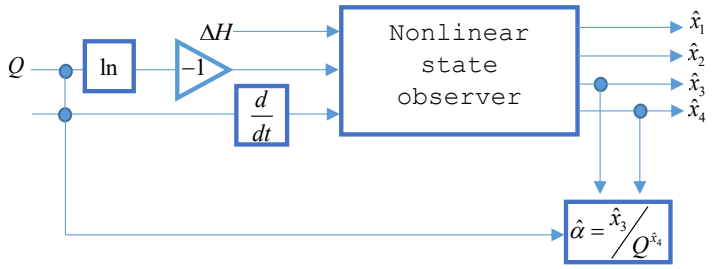


Fig. 8.1: Proposed approach

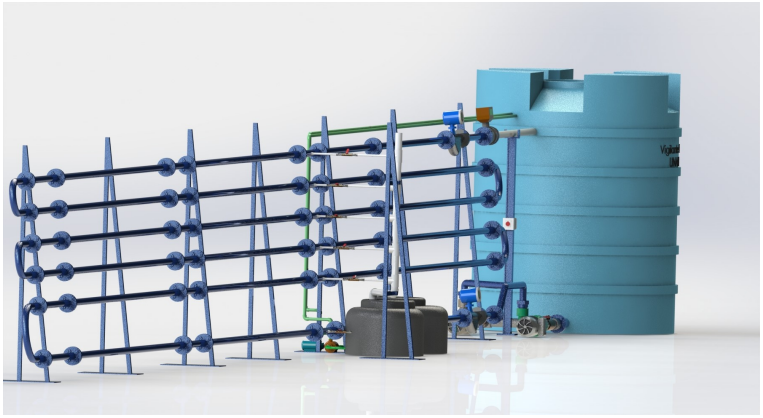

Fig. 8.2: Pipeline located at the hydrodynamics laboratory of II-UNAM

Table 8.1: Parameters of the laboratory pipeline

| Parameters | Values |
|---|---|
| $D$ [m] | 0.076 |
| $L$ [m] | 163.715 |
| $g$ [m/s$^2$] | 9.81 |
| $b$ [m/s] | 1330 |
| $\nu$ [m$^2$/s] | $10^{-6}$@20°C |

restrict the water flow. Two hydraulic pumps of variable speed fix the upstream boundary condition of the system: Pump 1 with a maximum power of 7.5 [HP] and Pump 2 with a maximum of 10 [HP]. Only Pump 1 was used here by changing the operation points with a variable frequency driver. Six valves are installed to emulate leaks or branches. The pipeline is instrumented with two flowmeters and two pressure sensors at the extremes. The Promass 83F flowmeters are based on the Coriolis principle with a maximum error of ±0.05%, while the Cerabar PMP71 pressure sensors are based on the deflection measurement of a diaphragm with a precision of 0.05%. All data during the experiments were sampled at 100 [ms].

In what follows, the description and analysis of each of the elements involved in the implementation and execution of the proposed method are presented.

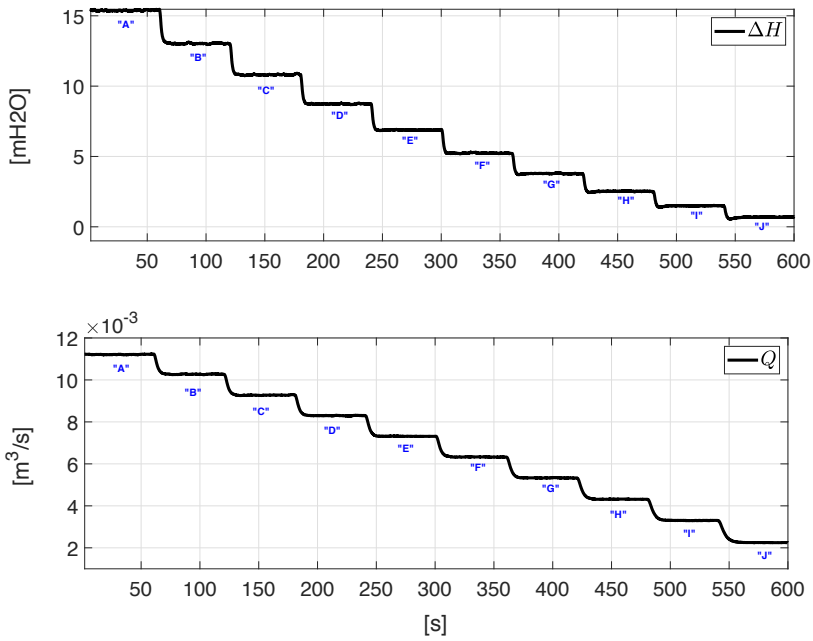


Fig. 8.3: Pressure head and flow rate recordings taken during the changes of operating point

### *8.4.1 Steady-state flow*

Table 8.2: Steady-state operating points (OPs)

| OP | $\bar{Q}$ [m$^3$/s] | $\overline{\Delta H}$ [mH2O] |
|---|---|---|
| A | 0.0112 | 15.3839 |
| B | 0.0103 | 13.0320 |
| C | 0.0093 | 10.8155 |
| D | 0.0083 | 8.7336 |
| E | 0.0073 | 6.8807 |
| F | 0.0063 | 5.2348 |
| G | 0.0053 | 3.7866 |
| H | 0.0043 | 2.5240 |
| I | 0.0033 | 1.4993 |
| J | 0.0022 | 0.6865 |

To capture and show the behavior of the head loss as a function of the flow rate, the pipeline was set at different operating points by manipulating the supply pump through a variable frequency drive. Figure 8.3 shows the recordings taken during the experiments: the flow rate, which was measured upstream in the pipeline, and the head loss calculated from pressure records measured upstream and downstream in the pipe. The staggered form of the recorded signals reveals how the change of operating points was performed: from the highest possible point when the pump operates at the electrical network's frequency to the lowest point when the flow measurement was still reliable. The operation points are labeled with the letter A, B, C,...,I. Once the data acquisition was concluded, the mean of the flow rate measurement at each operating point, denoted hereafter as $\bar{Q}$, was obtained as well as the mean of the head loss, denoted as $\overline{\Delta H}$. Table 8.2 contains the values of $\bar{Q}$ and $\overline{\Delta H}$.

### *8.4.2 Steady-oscillatory flow*

One way to generate steady-oscillatory flow in the laboratory pipeline is by injecting a sinusoidal signal into the pump's variable frequency drive (VFD). Taking this fact into account, two different steady-oscillatory flows were generated for testing the proposed calibration approach. The frequency of both sinusoidal signals injected into the pump's VFD was the same: $\omega = 0.1\pi$ [rad/s] (i.e. $f = 0.05$ [Hz]). The amplitude and offset of the hydraulic variables associated with both steady-oscillatory flows are listed in Table 8.3.

Figure 8.4 shows the head loss as a function of the flow rate for both the *high flow* and the *low flow*. This figure highlights the fact that oscillatory flows only cover a range of the total range of all the operating points used to show the head loss behavior. Figure 8.5 shows the derivative of the flow rate corresponding to the *high flow*.

Table 8.3: Features of the generated steady-oscillatory flows

| Variable | *Low flow* | *High flow* |
|---|---|---|
| $Q$ | Offset: 0.007351 [$m^3$/s]<br>Amplitude: 0.0032 [$m^3$/s] | Offset: 0.00932 [$m^3$/s]<br>Amplitude: 0.0032 [$m^3$/s] |
| $H_{in}$ | Offset: 11.15 [mH2O]<br>Amplitude: 8.192 [mH2O] | Offset: 16.02 [mH2O]<br>Amplitude: 9.75 [mH2O] |
| $H_{out}$ | Offset: 4.03 [mH2O]<br>Amplitude: 1.43 [mH2O] | Offset: 5.00 [mH2O]<br>Amplitude: 1.84 [mH2O] |

### *8.4.3 Tuning of the state observer*

Two estimations of the power-law parameters were performed. The first by using the *high flow* as the excitation and the second one by using the *low flow*. Both estimations were executed by using the same tuning parameters for the state observer (8.8). The observer was tuned by setting $\lambda = 1$. Its initial condi-

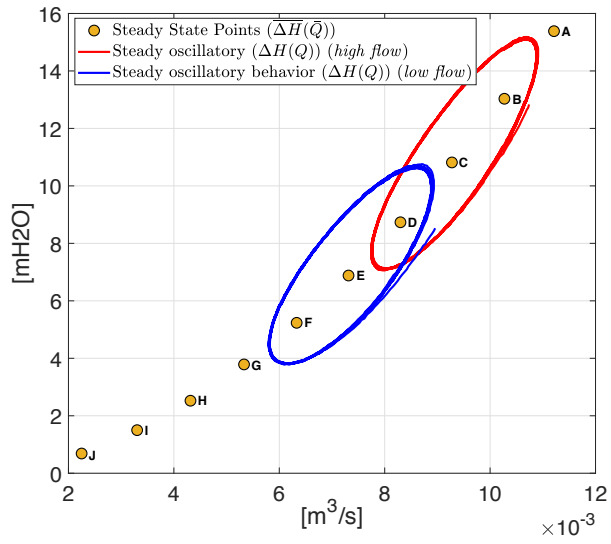


Fig. 8.4: Head loss versus flow rate in steady state and steady-oscillatory state

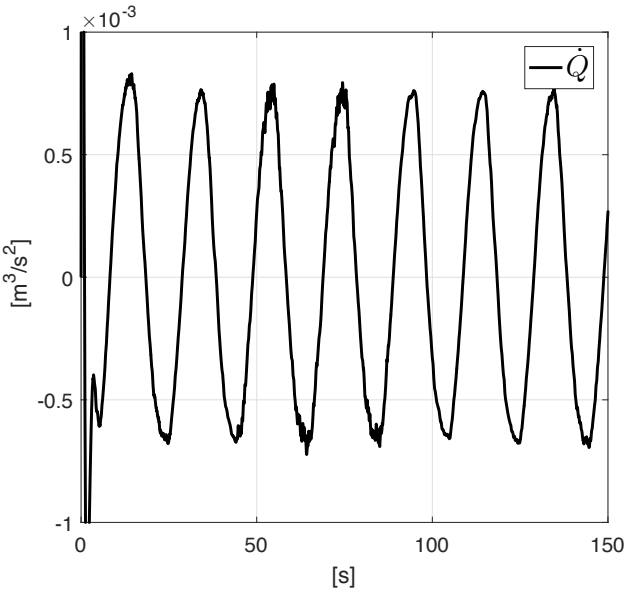


Fig. 8.5: $\dot{Q}$ in a time window of its computation for the *high flow*

tions were set as follows: $\hat{x}(0) = \begin{pmatrix} 0.12 & 0.001 & 0.01 & 0.08 \end{pmatrix}^T$ and $S(0) = I$. The observer was implemented in MATLAB/Simulink® by using the ODE3 solver with $\Delta t = 0.001$ [s] as the time step. Figure 8.6 shows the time evolution of $\hat{\beta}$ and $\hat{\gamma}$ for the *high flow* and the *low flow*. The means of the estimated parameters for the *high flow* and *low flow* were very close. In other words, the estimation results are slightly insensitive to the offset of the steady-oscillatory flow. Therefore, only the means corresponding to the *high flow* are considered in the rest of the discussion, which indeed resulted as follows: $\bar{\gamma} = 0.8897$,

$\bar{\beta} = 2.088 \times 10^{-4}$ and $\bar{\alpha} = 14.35$. A consequence of these values is $\bar{\Omega} = \bar{\alpha}/\bar{\beta} = 74569$, which is the coefficient of the estimated head loss given as $\widehat{\Delta H} = 74569 Q^{1.8897}$.

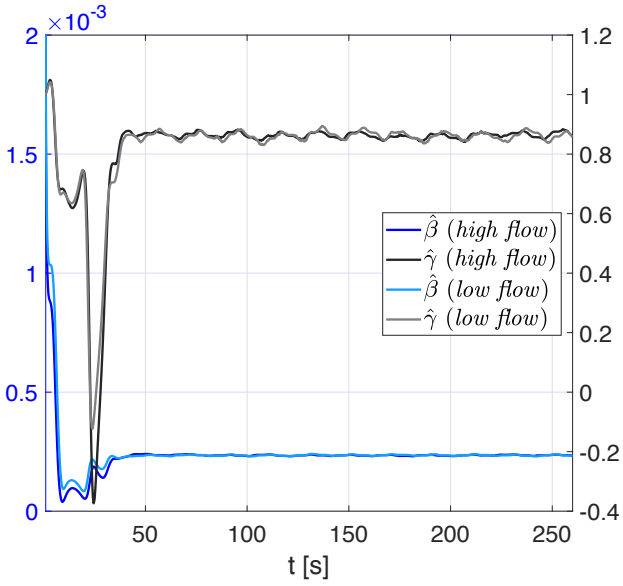


Fig. 8.6: Time evolution of $\hat{\beta}$ and $\hat{\gamma}$ by using the *high flow* and the *low flow* as excitation

## 8.5 Analysis of the results

In order to evaluate the performance of both the power law and the proposed algorithm, two evaluations were performed.

### *8.5.1 Model comparison*

The first is a comparison of the errors calculated from real data and several models of the head loss in steady state. These models are as follows: the Hazen-Williams (HW) formula, a quadratic equation without the linear term and a quadratic equation. The coefficients of the head loss models were also estimated by using state observers. The errors are calculated as the difference between the experimental data and the estimated with each formula, i.e., $e = \Delta H - \widehat{\Delta H}$. The resulting errors are presented in Table 8.4. The smallest errors are written in bold. Notice that the power law approximates with better accuracy the behavior of the head loss at almost all the operation points. To corroborate this fact, a visual comparison can be performed in Fig. 8.7, which concretely shows the estimated head loss (with each formula) normalized with respect to the real head loss. It is noticeable that the power law and the HW formula approximate with better accuracy the head loss behavior.

Table 8.4: Modeling errors

| OP | $\Omega Q^{\gamma+1}$ | $\theta_1 Q^2$ | $\theta_{11}Q^2+\theta_{21}Q$ | $\theta_2 Q^{1.852}$ |
|---|---|---|---|---|
| A | **2.4518e-06** | -0.3588 | -0.0541 | 0.0770 |
| B | **-0.0032** | -0.1789 | -0.0549 | 0.0191 |
| C | 0.0649 | 0.0419 | **0.0057** | 0.0420 |
| D | **0.0207** | 0.1086 | -0.0538 | -0.0345 |
| E | **0.0188** | 0.1820 | -0.0768 | -0.0577 |
| F | **0.0127** | 0.2175 | -0.1064 | -0.0744 |
| G | **0.0114** | 0.2275 | -0.1307 | -0.0765 |
| H | **-0.0078** | 0.1922 | -0.1681 | -0.0874 |
| I | **-0.0283** | 0.1332 | -0.1962 | -0.0924 |
| J | -0.0529 | **0.0527** | -0.2097 | -0.0952 |

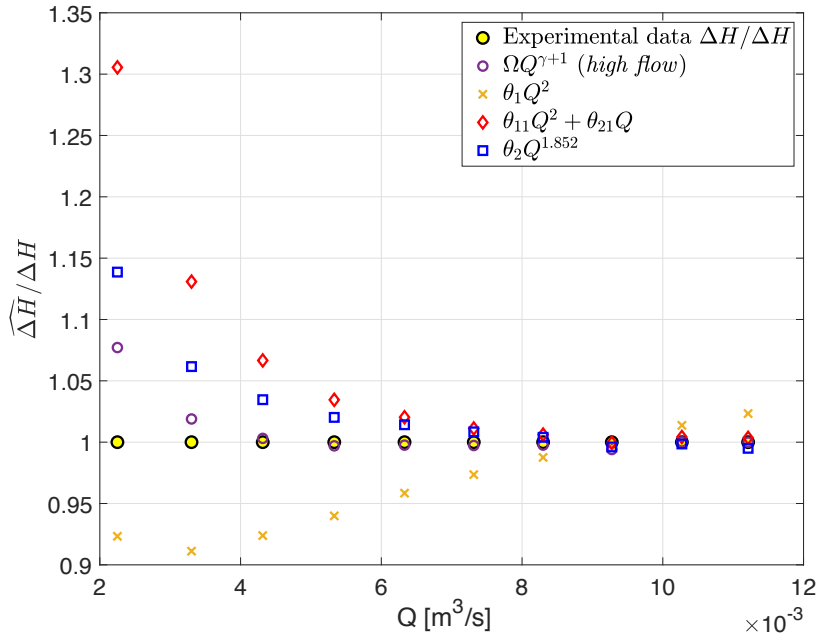


Fig. 8.7: Comparison of different head-loss models in steady state

The second evaluation is a comparison between the estimation results provided by the proposed approach and the results obtained with the next estimation methodology. The MATLAB instruction `fit` was used to find the parameters of the power law by interpolating the operation points B,C and D, which correspond to the same operation range of the oscillatory flow used for the estimation with the state observer: the *high flow*. Check Fig. 8.4 to verify this fact. The results were $\Omega_{fit} = 68730$ and $\gamma_{fit} = 0.8717$.

The relative errors of the fitting for each operation point by using both methods are displayed in Table 8.5. Note that the adjustment with the power law estimated with the proposed approach has small errors

Table 8.5: Approach errors

| OP | Online-based approach | MATLAB(B:D) |
|---|---|---|
| A | $\mathbf{2.451}\times10^{-6}$ | 0.0108 |
| B | **-0.0032** | -0.0146 |
| C | 0.0649 | **0.0358** |
| D | 0.0207 | **-0.0204** |
| E | **0.0188** | -0.0293 |
| F | **0.0127** | -0.0376 |
| G | **0.0114** | -0.0368 |
| H | **-0.0078** | -0.0498 |
| I | **-0.0283** | -0.0612 |
| J | **-0.0529** | -0.0741 |

in almost all points of operation, except points C and D. This fact is a clear evidence that the proposed method estimates accurately the values for the power law.

## 8.6 Relevance of head loss calibration in leak location

One of the requirements for implementing a model-based fault diagnosis system is to have a suitable and well-calibrated model. Furthermore, when we speak about calibration in the context of modeling and analysis of dynamic systems, we refer to the identification of systems, which is the process by which the parameters of a model are adjusted, using data measured from the real process. Thus, the error between the model and the process is the smallest possible using some metric.

In the context of *Fault Detection and Identification*, there are parameters or quantities that can most notably affect the diagnosis of a fault, so their estimation during calibration should be emphasized to obtain the best accurate diagnosis. In the case of leak detection and location, this quantity is head loss.

To verify the above remark, numerical simulations of a leak location algorithm based on a state observer were performed. The state observer is based on the model, which describes the flow in two different sections of the pipeline: the section to the left of the leak (namely $\Delta z = z_\ell - z_0$) where the head loss is $\Delta H = H_{in} - H_\ell$ and the section to the right of the leak (namely $\Delta z = L - z_\ell$) where the head loss is $\Delta H = H_\ell - H_{out}$:

$$\dot{Q}_{in} = \frac{\theta}{z_\ell - z_0}(H_{in} - H_\ell) - \alpha Q_{in}^{\gamma+1}, \tag{8.18}$$

$$\dot{Q}_{out} = \frac{\theta}{L - z_\ell}(H_\ell - H_{out}) - \alpha Q_{out}^{\gamma+1}. \tag{8.19}$$

where $Q_{in}$ and $Q_{out}$ are the inlet an outlet flow rates, respectively. $H_{in}$ and $H_{out}$ are the upstream and downstream hydraulic heads, respectively. $\theta = gA_r$, $\alpha$ is a factor involving the friction losses, $\gamma$ is the head loss exponent, $z_0 = 0$ is the origin coordinate (the upstream end) of the pipeline, $z_\ell$ is the leak coordinate (position) and $H_\ell$ is the pressure head at the leak junction.

If $H_\ell$ is replaced by any of the following equations obtained from (8.18) and (8.19) in steady state

$$H_\ell = H_{in} - \frac{\alpha}{\theta} Q_{in}^{\gamma+1} z_\ell, \;\; H_\ell = \frac{\alpha}{\theta} Q_{out}^{\gamma+1} (L - z_\ell) + H_{out}, \tag{8.20}$$

and by defining the following new state variables $x_1 = Q_{in} - Q_{out}$ and $x_2 = 1/z_\ell$, then the following second-order system can be obtained from (8.18) and (8.19):

$$\begin{aligned} \dot{x}_1 &= x_2 \left[ \theta (H_{in} - H_{out}) - L \left( \alpha Q_{out}^{\gamma+1} \right) \right] - \alpha \left( Q_{in}^{\gamma+1} - Q_{out}^{\gamma+1} \right), \\ \dot{x}_2 &= 0. \end{aligned} \tag{8.21}$$

Notice that (8.21) has the following general form:

$$\begin{aligned} \begin{bmatrix} \dot{x}_1 \\ \dot{x}_2 \end{bmatrix} &= \begin{bmatrix} 0 & u \\ 0 & 0 \end{bmatrix} \begin{bmatrix} x_1 \\ x_2 \end{bmatrix} + \begin{bmatrix} \varphi \\ 0 \end{bmatrix}, \\ y &= x_1, \end{aligned} \tag{8.22}$$

where $u = \left[ \theta (H_{in} - H_{out}) - L \left( \alpha Q_{out}^2 \right) \right]$ and $\varphi = -\alpha \left( Q_{in}^2 - Q_{out}^2 \right)$ are known smooth functions.

For system (8.22), the following state observer for locating single leaks was proposed in Torres et al. (2019):

$$\begin{aligned} \begin{bmatrix} \dot{\hat{x}}_1 \\ \dot{\hat{x}}_2 \end{bmatrix} &= \underbrace{\begin{bmatrix} 0 & u \\ 0 & 0 \end{bmatrix}}_{A} \begin{bmatrix} \hat{x}_1 \\ \hat{x}_2 \end{bmatrix} + \begin{bmatrix} \varphi \\ 0 \end{bmatrix} + \begin{bmatrix} K_1 \\ K_2 \end{bmatrix} e, \\ \hat{y} &= \underbrace{\begin{bmatrix} 1 & 0 \end{bmatrix}}_{C} \hat{x}, \end{aligned} \tag{8.23}$$

where $\hat{x}_1 = \hat{Q}_{in} - \hat{Q}_{out}$ and $\hat{x}_2 = 1/\hat{z}_\ell$ are the states to be estimated. Moreover, $e = y - \hat{x}_1$ is the observation error. $K_1$ and $K_2$ are elements of the gain vector $K$, which can be calculated as follows: $K = S^{-1} C^T$, where $S$ is the solution of the following matrix Lyapunov differential equation:

$$\dot{S} = -\lambda S - A^T S - SA + C^T C, \tag{8.24}$$

with $\lambda > 0$ and $S(0) > 0$.

To recover the estimation of the leak position from the state observer, $\hat{x}_2$ must be inverted: $\hat{z}_\ell = 1/\hat{x}_2$.

The fundamental objective of the numerical simulations was to investigate the result of the leak location by taking into account uncertainty in the parameter $\alpha$, which is a key quantity used for describing the head loss in a duct.

The uncertainty was modeled by a uniform probability density function (p.d.f.) given by $\mathscr{U}(a,b)$, where $a \sim \alpha - 0.2\alpha$ and $b \sim \alpha + 0.2\alpha$. A histogram of the p.d.f. for $\alpha$ is given in Fig. 8.8.

The leaks were simulated at four different positions: $z_\ell = [122.79 \quad 81.86 \quad 40.93 \quad 20.465]$ (m), where $L = 163.72$ (m) is the total length of the simulated pipeline. The rest of the physical parameters used to simulate the pipeline are given in Table 8.1.

The results of the leak location with friction uncertainty for the different position cases are summarized in Table 8.6, which shows the estimate clearly deviates when the value of $\alpha$ is not exactly known. On

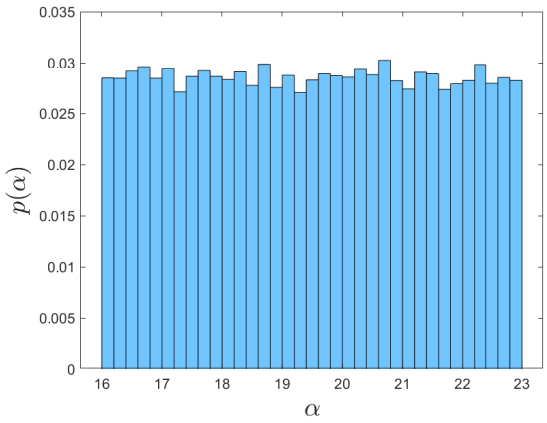


Fig. 8.8: $\alpha$ uncertainty distribution

the contrary, in Fig. 8.9 is shown that the true leak position's values are estimated when there is no uncertainty in friction.

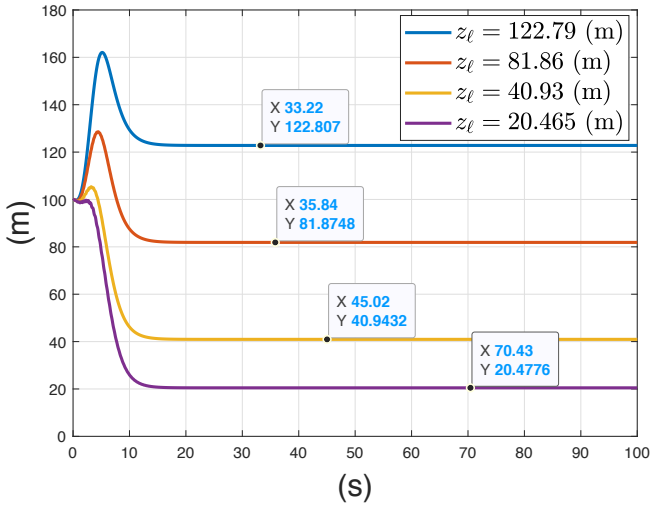


Fig. 8.9: Leak position estimation with the true value for $\mu$

Table 8.6: Mean and standard deviation of the leak position estimations

| **Leak position** (m) | **Mean** (m) | **Standard Deviation** (m) |
|---|---|---|
| 20.465 | 20.36 | 8.52 |
| 40.93 | 40.41 | 7.20 |
| 81.86 | 80.70 | 5.30 |
| 122.79 | 120.917 | 5.07 |

## 8.7 Conclusions

This chapter has proposed a method based on the rigid water column model to calibrate the parameters of a power law that describes the head loss of a pipeline. The method can be applied using real-time information from, for example, SCADA or IoT systems. Some advantages of the proposed method are listed below.

- The method permits calibrating a head loss model with only two parameters to be identified, instead of calibrating a model with more than two parameters, such as the DW equation or the HW formula.
- The method is an alternative to calibrate a head loss model even though the physical parameters of the pipeline, such as roughness or the cross-sectional area, are unknown.
- It allows finding a good set of parameters so that the power-law model can be adjusted accurately to the head loss curve. Regarding this advantage, a comparison between the parameter estimation was presented with the new proposition and the offline least squares algorithm performed using MATLAB.
- It provides similar results regardless of the pipeline operation region in which the oscillatory flow is generated for the calibration.
- The method provides a good set of parameters so that the power-law model accurately describes the head loss at all the operating points, regardless of whether the oscillatory flow has been generated around an operating point in a small region. This is an advantage over other methods that require information (pressure and flow rate) from all the operation points to obtain a satisfactory set of parameters.
- It can be applied to a long pipeline by measuring pressure at two different pipeline coordinates delimiting a short section of the pipeline.
- It can be used online together with leak diagnosis algorithms.

# References


Adamkowski, A. and Lewandowski, M. (2006). Experimental examination of unsteady friction models for transient pipe flow simulation. *Journal of Fluids Engineering*, 128(6):1351–1363.

Bergant, A., Ross Simpson, A., and Vìtkovsk, J. (2001). Developments in unsteady pipe flow friction modelling. *Journal of Hydraulic Research*, 39(3):249–257.

Besançon, G. (2007). *Nonlinear Observers and Applications*. Springer.

Besançon, G. (2016). A link between output time derivatives and persistent excitation for nonlinear observers. *IFAC-PapersOnLine*, 49(18):493–498.

Brkić, D. (2011). Review of explicit approximations to the Colebrook relation for flow friction. *Journal of Petroleum Science and Engineering*, 77(1):34–48.

Cabrera, E., Garcia-Serra, J., and Iglesias, P. L. (1995). Modelling water distribution networks:from steady flow to water hammer. In *Improving effic. & reliability in water distribution syst.*, pages 3–32. Springer.

Chaudhry, M. H. (1979). *Applied Hydraulic Transients*. New York: Van Nostrand Reinhold.

Datta, R. and Sridharan, K. (1994). Parameter estimation in water-distribution systems by least squares. *Journal of Water Resources Planning and Management*, 120(4):405–422.

Díaz, S., Mínguez, R., and González, J. (2017). Calibration via multi-period state estimation in water distribution systems. *Water resources management*, 31(15):4801–4819.

Farshad, F. F., Pesacreta, T. C., Garber, J. D., and Bikki, S. (2001). A comparison of surface roughness of pipes as measured by two profilometers and atomic force microscopy. *Scanning*, 23(4):241–248.

Gao, T. (2017). Roughness and demand estimation in water distribution networks using head loss adjustment. *Journal of Water Resources Planning and Management*, 143(12):04017070.

Hitzer, E. (2001). Early works on the Hagen-Poiseuille flow. *Memoirs-faculty of Engineering Fukui University*, 49(1):45–54.

Islam, M. R. and Chaudhry, M. H. (1998). Modeling of constituent transport in unsteady flows in pipe networks. *Journal of Hydraulic Engineering*, 124(11):1115–1124.

Kumar, S. M., Narasimhan, S., and Bhallamudi, S. M. (2010). Parameter estimation in water distribution networks. *Water resources management*, 24(6):1251–1272.

Larock, B. E., Jeppson, R. W., and Watters, G. Z. (1999). *Hydraulics of pipeline systems*. CRC press.

Liou, C. P. (1998). Limitations and proper use of the Hazen-Williams equation. *Journal of Hydraulic Engineering*, 124(9):951–954.

Moore, W. (1959) Relationships between pipe resistance formulas. *Journal of the Hydraulics Division*. 85(3): 25–41

Nault, J. and Karney, B. (2016). Improved rigid water column formulation for simulating slow transients and controlled operations. *Journal of Hydraulic Engineering*, 142(9):04016025.

Ostfeld, A., Salomons, E., Ormsbee, L., Uber, J. G., Bros, C. M., Kalungi, P., Burd, R., Zazula-Coetzee, B., Belrain, T., Kang, D., et al. (2011). Battle of the water calibration networks. *Journal of Water Resources Planning and Management*, 138(5):523–532.

Puig, V., Ocampo-Martínez, C., Pérez, R., Cembrano, G., Quevedo, J., and Escobet, T. (2017). *Real-time Monitoring and Operational Control of Drinking-Water Systems*. Springer.

Reddy, P. N., Sridharan, K., and Rao, P. (1996). WLS method for parameter estimation in water distribution networks. *Journal of Water Resources Planning and Management*, 122(3):157–164.

Rojas, J., Verde, C., and Torres, L. (2018). On-line head loss identification for monitoring of pipelines. In *10th IFAC Symposium on Fault Detection, Supervision and Safety for Technical Processes*, Warsaw, Poland.

Savic, D. A., Kapelan, Z. S., and Jonkergouw, P. M. (2009). Quo vadis water distribution model calibration? *Urban Water Journal*, 6(1):3–22.

Scola, I. R., Besançon, G., and Georges, D. (2018). Optimizing Kalman optimal observer for state affine systems by input selection. *Automatica*, 93:224–230.

Sletfjerding, E. and Gudmundsson, J. S. (2003). Friction factor directly from roughness measurements. *Journal of energy resources technology*, 125(2):126–130.

Torres, L., Besancon, G., and Georges, D. (2012). EKF-like observer with stability for a class of nonlinear systems. *IEEE Transactions on Automatic Control*, 57(6):1570–1574.

Torres, L. and Verde, C. (2018). Nonlinear estimation of a power law for the friction in a pipeline. *IFAC-PapersOnLine*, 51(13):67–72.

Torres, L., Verde, C., and Rojas, J. (2019). Minimal-order observers for locating leaks in a pipeline with a branch. *IFAC-PapersOnLine*, 52(23):67–72.

Verde, C. and Torres, L. (2017). *Modeling and Monitoring of Pipelines and Networks: Advanced Tools for Automatic Monitoring and Supervision of Pipelines*, volume 7. Springer.

White, F. M. (1999). Fluid mechanics, wcb. *Ed McGraw-Hill Boston*.

Xu, X. and Karney, B. (2017). An overview of transient fault detection techniques. *Modeling and monitoring of pipelines and networks*, pages 13–37.